



Measurement of $\phi(1020)$ meson production in fixed-target $p\text{Ne}$ collisions at $\sqrt{s_{\text{NN}}} = 68.5 \text{ GeV}$

LHCb collaboration[†]

Abstract

The first measurement of $\phi(1020)$ meson production in fixed-target $p\text{Ne}$ collisions at $\sqrt{s_{\text{NN}}} = 68.5 \text{ GeV}$ is presented. The $\phi(1020)$ mesons are reconstructed in their K^+K^- decay in a data sample consisting of proton collisions on neon nuclei at rest, corresponding to an integrated luminosity of $21.7 \pm 1.4 \text{ nb}^{-1}$, collected by the LHCb detector at CERN. The $\phi(1020)$ production cross-section in the centre-of-mass rapidity range of $-1.8 < y^* < 0$ and transverse momentum range of $800 < p_{\text{T}} < 6500 \text{ MeV}/c$ is found to be $\sigma = 182.7 \pm 2.7 \text{ (stat.)} \pm 14.1 \text{ (syst)} \mu\text{b/nucleon}$. A double-differential measurement of the cross-section is also provided in four regions of rapidity and six regions of transverse momentum of the $\phi(1020)$ meson and compared with the predictions from Pythia and EPOS4, which are found to underestimate the experimental values.

Submitted to JHEP

© 2024 CERN for the benefit of the LHCb collaboration. [CC BY 4.0 licence](#).

[†]Authors are listed at the end of this paper.

1 Introduction

The existence of a quark-gluon plasma (QGP), a state of matter where quarks and gluons are deconfined, is allowed by quantum chromodynamics (QCD) at high temperature and high baryon density [1]. Experimental evidence of QGP formation has been found in large collision systems [2–4], while formation of QGP droplets has been proposed to describe some observables in collisions of small asymmetric systems (*e.g.* proton-nucleus) at $\sqrt{s_{\text{NN}}} = 200$ GeV [5]. However, in proton-nucleus collisions, cold nuclear matter (CNM) effects are also present, such as modifications of the initial parton distribution functions in nuclei (nPDFs) due to shadowing [6, 7], energy loss [8] and nuclear breakup [9, 10], which produce effects similar to QGP. The study of particle production in small systems is thus crucial to disentangle CNM effects from the possible formation of QGP at temperature and density lower than it is generally expected [11].

One of the signatures of QGP formation is the enhancement of strange-hadron production as a result of the chemical equilibrium of strange quarks [12]. This enhancement has been observed in a variety of collision systems [13–15]. The $\phi(1020)$ meson, hereafter referred to as ϕ , is abundantly produced at the LHC because it is a light bound state of a strange quark-antiquark pair. The ϕ meson production in ordinary matter is suppressed due to the Okubo–Zweig–Iizuka (OZI) rule compared to other vector mesons of similar mass [16–18]. In the QGP medium, ϕ mesons can instead be produced through the coalescence of abundant strange quarks, bypassing the OZI rule. This increase makes the ϕ meson an ideal probe of QGP [19]. Alternative mechanisms to QGP formation such as string fusion [20], colour reconnection [21] and rope hadronisation [22] have also been proposed to describe strangeness enhancement. Hence, studying ϕ meson production in proton-nucleus collisions at different centre-of-mass energies is essential to provide insights into this complex variety of scenarios.

This paper presents the first measurement of ϕ meson production in proton-neon ($p\text{Ne}$) fixed-target collisions at $\sqrt{s_{\text{NN}}} = 68.5$ GeV by the LHCb experiment. The differential production cross-section is measured as a function of the ϕ meson transverse momentum p_{T} , and rapidity in the centre-of-mass of the reaction y^* .

2 The LHCb detector and the SMOG system

The LHCb detector [23, 24] is a single-arm forward spectrometer designed for studying particles containing c or b quarks, covering the pseudorapidity range $2 < \eta < 5$. The detector comprises a silicon-strip vertex locator (VELO), three tracking stations equipped with silicon-strip detectors and straw drift tubes, two ring-imaging Cherenkov (RICH) detectors for charged hadron identification, a calorimeter system with scintillating-pad and preshower detectors, electromagnetic and hadronic calorimeters, and a muon detector with alternating layers of iron and multiwire proportional chambers.

The System for Measuring the Overlap with Gas (SMOG) [25] enables the injection of gases (He, Ar, Ne) at pressures of $\mathcal{O}(10^{-7})$ mbar into the beam pipe section within the VELO, allowing LHCb to operate as a fixed-target experiment. This provides a unique opportunity to study proton-nucleus and nucleus-nucleus collisions with different gaseous targets using the LHC beams. In this configuration, the high-energy proton beam allows the LHCb acceptance to extend into the negative rapidity hemisphere in the

nucleon-nucleon centre-of-mass system of the reaction, covering the region from $y^* \sim -2.5$ to $y^* \sim 0$.

3 Data sample and simulation

The $p\text{Ne}$ sample was collected in 2017 simultaneously with the proton-proton (pp) collision data, where a beam of protons with an energy of 2.51 TeV collided against neon nuclei at rest, resulting in a centre-of-mass energy of $\sqrt{s_{\text{NN}}} = 68.5$ GeV.

Simulated samples of $\phi \rightarrow K^+K^-$ decays are generated with PYTHIA [26], configured specifically for LHCb [27], with the colliding proton beam momentum set to match the momentum per nucleon of both the beam and the target in the centre-of-mass frame. The four-momentum of the ϕ decay products is then embedded into $p\text{Ne}$ minimum bias events generated by the EPOS-LHC event generator [28]. The interaction of the generated particles with the detector, along with its response, are simulated using the GEANT4 toolkit [29, 30], as described in Ref. [31]. The simulated samples are reconstructed and analysed using the same software tools employed for data processing.

4 Event selection

The proton-gas events are selected by a two-stage trigger [32]. The first stage is hardware-based and selects a constant rate of proton bunches moving towards the detector. These bunches do not cross any filled bunch moving in the opposite direction at the nominal pp interaction point. The second stage is software-based and selects events with at least one track in the VELO. In addition, to suppress residual pp collisions, events with activity in the backward region are vetoed based on the number of tracks in VELO stations upstream of the interaction region.

In the offline selection, the ϕ candidates are formed from two opposite-charge kaon tracks forming a good-quality vertex close to the primary $p\text{Ne}$ collision vertex (PV). Each kaon track is required to have a minimum momentum of 2 GeV/ c and a minimum transverse momentum of 400 MeV/ c , and the selected pairs should have an invariant mass between 990 and 1100 MeV/ c^2 . Tight particle identification (PID) requirements are applied to select kaons. The measurement is performed in the ϕ transverse momentum range $800 < p_T < 6500$ MeV/ c and centre-of-mass rapidity range $-1.8 < y^* < 0$. The z coordinate of the PV is required to lie in the interval $z_{\text{PV}} \in [-200, -100] \cup [100, 150]$ mm to suppress the contamination from pp collisions that occur at $z_{\text{PV}} \sim 0$ mm.

Figure 1 shows the K^+K^- invariant-mass distribution of the selected candidates. The fit function is also shown and is composed of a background and a signal component. The background is described with a second-order polynomial function, where the coefficients are free to vary. The signal is described with a relativistic Breit–Wigner function,

$$f_{\text{sig}}(m) = \frac{m\Gamma(m)}{(m^2 - m_\phi^2)^2 + m_\phi^2\Gamma^2(m)}, \quad (1)$$

where

$$\Gamma(m) = \Gamma_\phi \frac{m}{m_\phi} \left[\frac{m^2/4 - m_K^2}{m_\phi^2/4 - m_K^2} \right]^{3/2}. \quad (2)$$

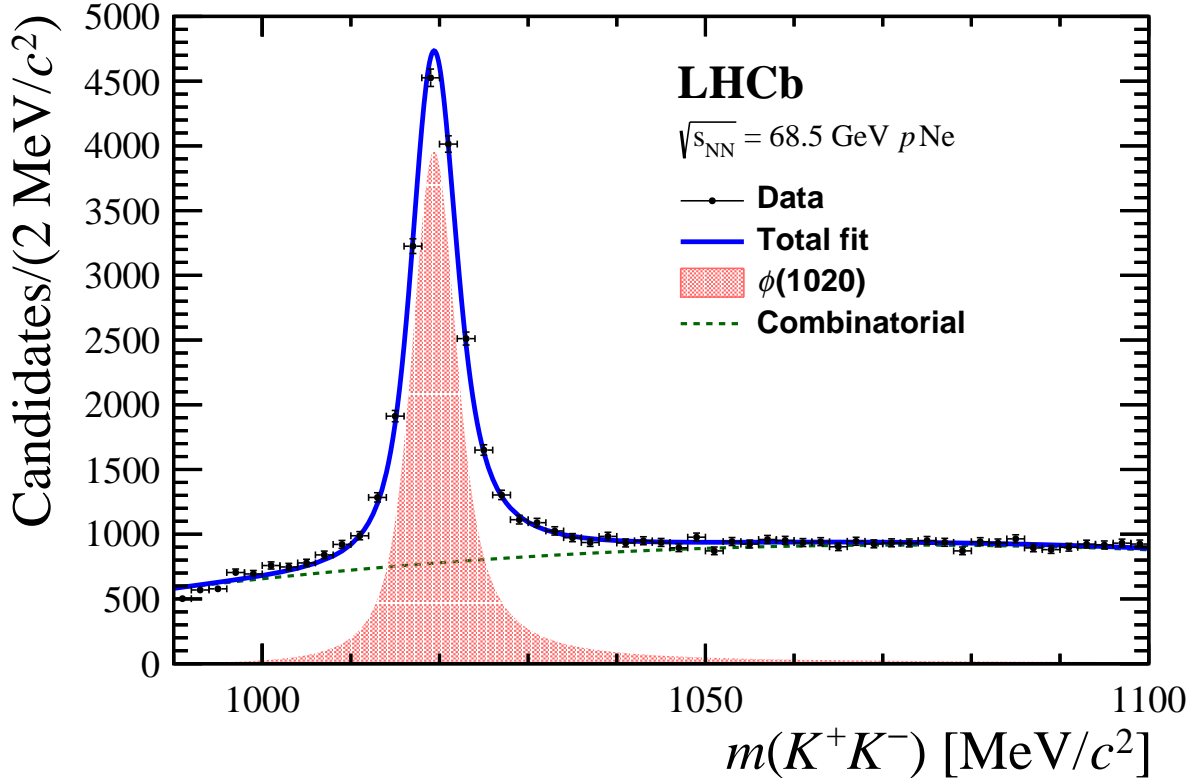


Figure 1: Invariant-mass distribution of $\phi \rightarrow K^+K^-$ candidates after the selection. The fit curve (solid blue line) is composed of combinatorial background (dashed green line) and signal (red area).

In the fit, m_K , m_ϕ and Γ_ϕ parameters are fixed to the known values [33]. To account for detector resolution effects, Eq. 1 is convolved with a Gaussian function whose width is free to vary in the fit. A total of 16866 ± 185 signal events are obtained from the unbinned maximum-likelihood fit to the K^+K^- invariant mass (m).

The double-differential cross-section per target nucleon is estimated by correcting the signal yield in each kinematic region, $N(p_T, y^*)$, obtained from independent fits, for the $\phi \rightarrow K^+K^-$ decay branching fraction $\mathcal{B}(\phi \rightarrow K^+K^-) = 49.1 \pm 0.5\%$ [33], the integrated luminosity of the sample \mathcal{L} , and the total efficiency $\epsilon_{\text{tot}}(p_T, y^*)$ according to the formula

$$\frac{d^2\sigma}{dp_T dy^*} = \frac{1}{\Delta p_T \Delta y^* \epsilon_{\text{tot}}(p_T, y^*) \cdot \mathcal{L} \cdot \mathcal{B}(\phi \rightarrow K^+K^-) \cdot A}, \quad (3)$$

where Δp_T and Δy are the kinematic region widths and $A = 20.18$ is the atomic weight of neon [34]. The total efficiency includes the geometrical acceptance of the detector and the efficiency of trigger, event reconstruction and offline selection.

The PV reconstruction efficiency is measured using a $\phi \rightarrow K^+K^-$ data sample reconstructed without vertex requirements [35]. The PID efficiency is estimated from a $\phi \rightarrow K^+K^-$ data sample where one of the two kaons (the *tag*) is selected with a tight PID requirement, while the other one (the *probe*) is selected without any PID condition. The efficiency for K^+ and K^- is defined as the fraction of ϕ candidates in which the probe track

passes the PID condition, which is estimated from an invariant-mass fit. The remaining efficiencies are computed from simulated samples, where events are assigned weights to ensure that the distribution of VELO cluster multiplicity matches that observed in data. Data corrections from pp calibration samples are also applied when estimating the track reconstruction efficiency. The integrated luminosity is determined to be $21.7 \pm 1.4 \text{ nb}^{-1}$ from the elastic proton scattering on neon atomic electrons [36].

5 Systematic uncertainties

Several sources of systematic uncertainty are considered, including those associated with the signal and background fit models, as well as with the evaluation of the efficiencies.

A systematic uncertainty is evaluated by computing the relative difference between the signal yield obtained with the baseline fit model and an alternative model based on an exponential function for the background and a Breit–Wigner function for the signal that includes the Blatt–Weisskopf barrier factors. These factors modify the mass-dependent signal width (Eq. 2) into

$$\Gamma(m) = \Gamma_\phi \frac{m}{m_\phi} \left[\frac{m^2/4 - m_K^2}{m_\phi^2/4 - m_K^2} \right]^{3/2} \frac{1 + r_0^2 (m_\phi^2/4 - m_K^2)}{1 + r_0^2 (m^2/4 - m_K^2)}, \quad (4)$$

where the radius of the ϕ meson is fixed to $r_0 = 5.1 \text{ GeV}^{-1}$ [33].

The uncertainty on the geometrical acceptance is due to the limited size of the simulated sample. An alternative set of weights to correct the multiplicity in the simulation is obtained using the number of tracks in the event instead of the number of VELO clusters. The difference between the efficiencies computed with this set of weights and the nominal efficiencies is assigned as a systematic uncertainty. The uncertainty on the PV reconstruction and PID efficiencies arise from the size of the individual data sample used for each estimate. The uncertainty on the reconstruction and selection efficiency depends on both the size of the simulated sample and the uncertainty on the tracking corrections obtained from data [37]. An additional source of systematic uncertainty arises from the contamination of residual pp collisions, which is evaluated from the comparison of data samples of pure $p\text{Ne}$ and pure pp collisions [38]. Finally, the uncertainty on the $\phi \rightarrow K^+K^-$ branching ratio and on the estimate of the integrated luminosity are also considered.

The sources and the corresponding uncertainty values are summarised in Table 1, separated between those correlated and uncorrelated across the kinematic regions.

6 Results

The measured ϕ production cross-section in $p\text{Ne}$ fixed-target collisions at $\sqrt{s_{\text{NN}}} = 68.5 \text{ GeV}$ within $-1.8 < y^* < 0$ and $800 < p_{\text{T}} < 6500 \text{ MeV}/c$ is found to be

$$\sigma = 182.7 \pm 2.7 \text{ (stat.)} \pm 14.1 \text{ (syst.) } \mu\text{b/nucleon.}$$

The double-differential cross-section is shown in Fig. 2, in different rapidity ranges as a function of p_{T} . The cross-section shows a decreasing trend with increasing momentum

Table 1: Summary of the relative contributions to the systematic and statistical uncertainties for this measurement. Correlated systematic uncertainties affect all kinematic regions by the same amount, while ranges denote the minimum and maximum values among the p_T and y^* regions.

Systematic uncertainties	
Uncorrelated among kinematic regions	
Signal determination	(<0.1 – 5.9)%
Geometrical acceptance	(<0.1 – 1.8)%
Multiplicity corrections	(0.2 – 3.6)%
PID efficiency	(2.3 – 4.4)%
Correlated among kinematic regions	
PV reconstruction	1.2%
Reconstruction and selection efficiency	3.2%
pp contamination	2.0%
$\mathcal{B}(\phi \rightarrow K^+ K^-)$	1.0%
Luminosity	6.5%
Statistical uncertainty	(3.7 – 6.7)%

and large negative rapidity, as observed for charmed mesons with the same energy and collision system [38]. By integrating the results, the single-differential cross-sections as a function of p_T and y^* are obtained and shown in Fig. 3 together with the predictions from Pythia 8.312 [39] and from a preliminary EPOS4 release [40–43]. This version of Pythia includes the Angantyr model [44], which can simulate pp , pA , and AA collisions, and offers the flexibility to modify the initial-state geometry model to accommodate light nuclei such as neon. In comparison, the preliminary release of EPOS4 provides pregenerated tables specifically for pNe collisions at $\sqrt{s_{NN}} = 68.5$ GeV. The strong p_T dependence is reproduced by the models, although they generally underestimate the data in almost all intervals.

The numerical values of the cross-section are reported in Tables 2 and 3. The average transverse momentum in each centre-of-mass rapidity region is provided in Table 4.

7 Conclusions

The first measurement of the production cross-section of the $\phi(1020)$ meson in pNe collisions at $\sqrt{s_{NN}} = 68.5$ GeV by the LHCb experiment is presented. The cross-section in the range of rapidity $-1.8 < y^* < 0$ and transverse momentum $800 < p_T < 6500$ MeV/ c is found to be

$$\sigma = 182.7 \pm 2.7 \text{ (stat.)} \pm 14.1 \text{ (syst.) } \mu\text{b/nucleon,}$$

where the first uncertainty is statistical, and the second is systematic. The differential cross-section is compared to predictions based on Pythia 8.312 and preliminary EPOS4 generators, which generally underestimate the experimental points. This result provides useful information to tune phenomenological models on strangeness production and will constitute a key reference for QGP searches in heavier colliding systems.

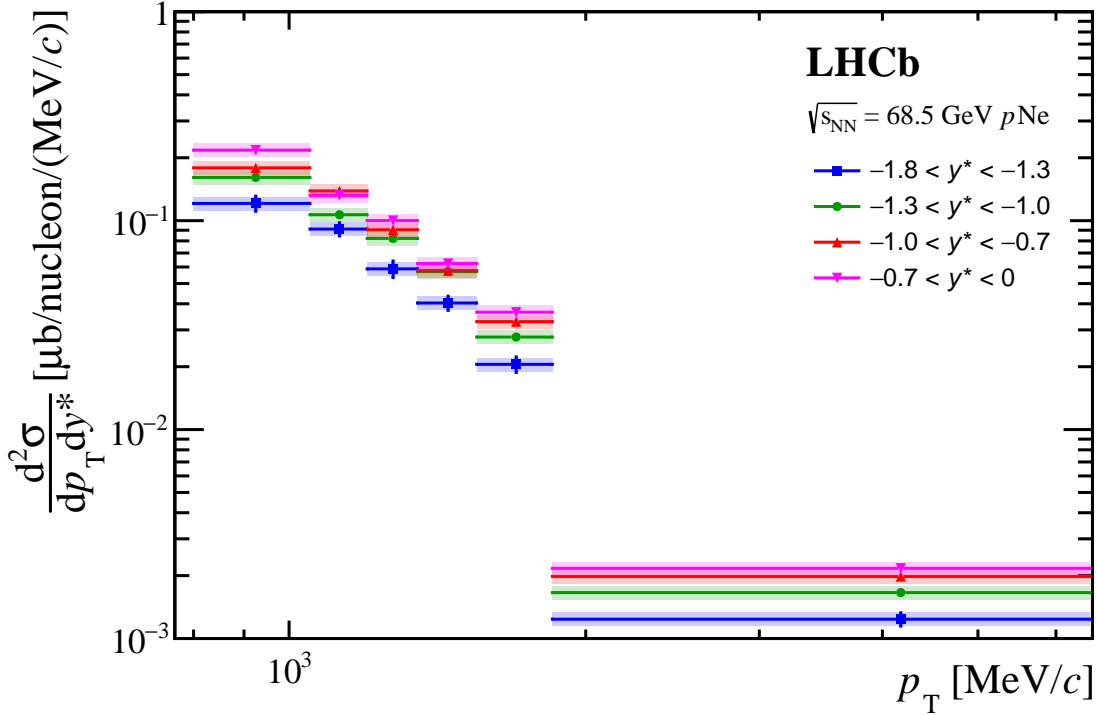


Figure 2: Double-differential ϕ -meson production cross-section per nucleon. Statistical and uncorrelated uncertainties are indicated by the bars, while the filled area represents the correlated uncertainty.

Table 2: Double-differential cross-section per nucleon as a function of (p_T, y^*) in units of $\mu\text{b}/\text{nucleon}/(\text{MeV}/c)$. The first uncertainty includes the statistical and uncorrelated contributions, while the second represents the correlated uncertainty.

Range p_T [MeV/c]	y^*	
	[-1.8, -1.3]	[-1.3, -1.0]
[800, 1050]	$0.121 \pm 0.010 \pm 0.009$	$0.161 \pm 0.012 \pm 0.012$
[1050, 1200]	$0.091 \pm 0.007 \pm 0.007$	$0.107 \pm 0.008 \pm 0.008$
[1200, 1350]	$0.059 \pm 0.005 \pm 0.004$	$0.082 \pm 0.006 \pm 0.006$
[1350, 1550]	$0.040 \pm 0.003 \pm 0.003$	$0.057 \pm 0.004 \pm 0.004$
[1550, 1850]	$0.021 \pm 0.002 \pm 0.002$	$0.028 \pm 0.002 \pm 0.002$
[1850, 6500]	$0.0012 \pm 0.0001 \pm 0.0001$	$0.0017 \pm 0.0001 \pm 0.0001$

Range p_T [MeV/c]	y^*	
	[-1.0, -0.7]	[-0.7, 0.0]
[800, 1050]	$0.179 \pm 0.013 \pm 0.014$	$0.218 \pm 0.013 \pm 0.014$
[1050, 1200]	$0.139 \pm 0.011 \pm 0.011$	$0.132 \pm 0.008 \pm 0.010$
[1200, 1350]	$0.090 \pm 0.006 \pm 0.007$	$0.100 \pm 0.006 \pm 0.008$
[1350, 1550]	$0.058 \pm 0.005 \pm 0.004$	$0.062 \pm 0.004 \pm 0.005$
[1550, 1850]	$0.033 \pm 0.002 \pm 0.003$	$0.036 \pm 0.003 \pm 0.003$
[1850, 6500]	$0.0020 \pm 0.0002 \pm 0.0002$	$0.0022 \pm 0.0001 \pm 0.0002$

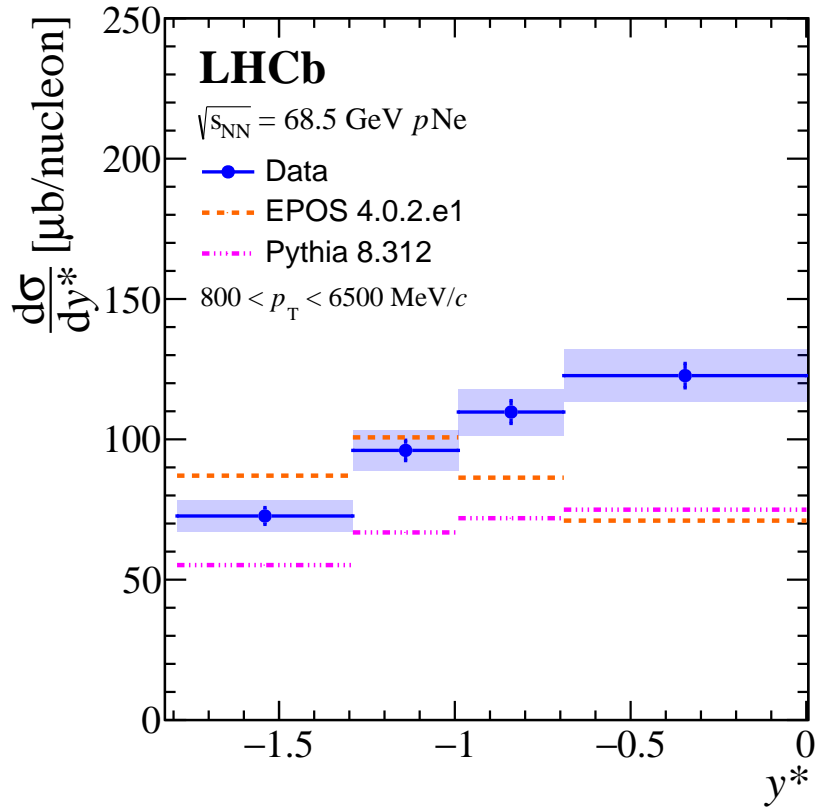
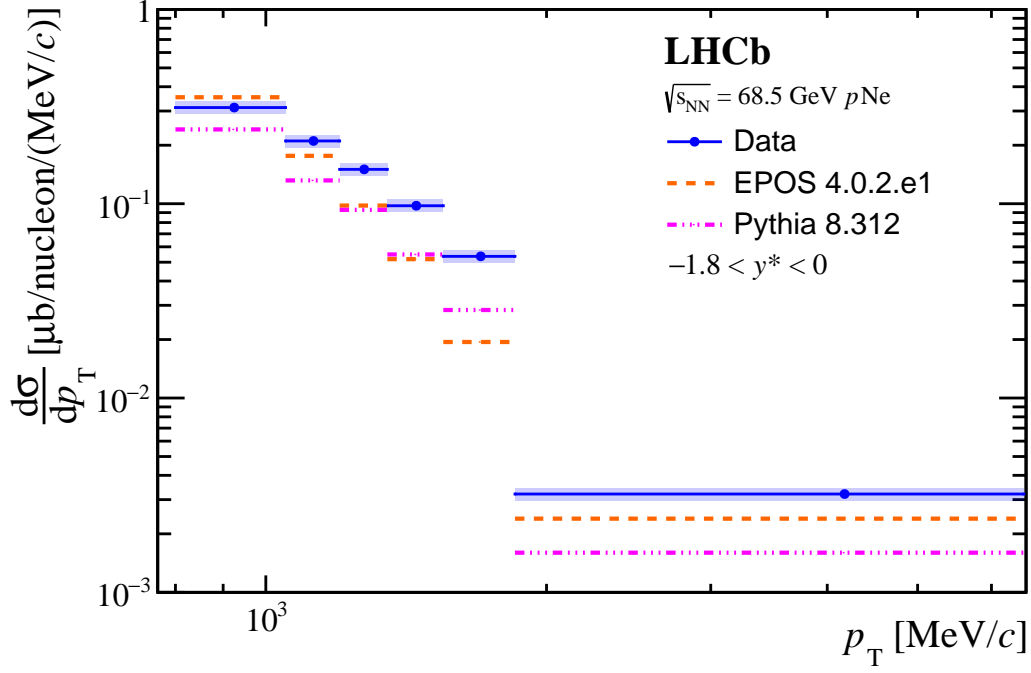


Figure 3: Single-differential cross-sections per nucleon (blue) as a function of (top) p_T in $-1.8 < y^* < 0$, and (bottom) y^* in $800 < p_T < 6500 \text{ MeV}/c$. The measurement are compared to EPOS4 (orange) and Pythia 8.312 (magenta) predictions. On the measurement, statistical and uncorrelated uncertainties are indicated by the bars, while the filled area represents the correlated uncertainty.

Table 3: Single-differential cross-section as a function of p_T or y^* . The first uncertainty includes the statistical and uncorrelated contributions, while the second represents the correlated uncertainty.

Range	Values
p_T [MeV/c]	$d\sigma/dp_T$ [$\mu\text{b}/\text{nucleon}/(\text{MeV}/c)$]
[800, 1050]	$0.313\pm 0.013\pm 0.024$
[1050, 1200]	$0.210\pm 0.008\pm 0.016$
[1200, 1350]	$0.150\pm 0.006\pm 0.011$
[1350, 1550]	$0.098\pm 0.004\pm 0.007$
[1550, 1850]	$0.054\pm 0.002\pm 0.004$
[1850, 6500]	$0.0032\pm 0.0001\pm 0.0002$
y^*	$d\sigma/dy^*$ [$\mu\text{b}/\text{nucleon}$]
[-1.8, -1.3]	$72.7\pm 3.0\pm 5.5$
[-1.3, -1.0]	$96.1\pm 3.6\pm 7.3$
[-1.0, -0.7]	$109.7\pm 4.1\pm 8.3$
[-0.7, 0.0]	$122.7\pm 4.3\pm 9.3$

Table 4: Average p_T in MeV/c units of the ϕ meson in each kinematic region and in the full rapidity range (last column).

Range p_T [MeV/c]	y^*				y^*
	[-1.8, -1.3]	[-1.3, -1.0]	[-1.0, -0.7]	[-0.7, 0.0]	[-1.8, 0.0]
[800, 1050]	961	965	951	964	960
[1050, 1200]	1125	1125	1126	1127	1126
[1200, 1350]	1274	1274	1272	1274	1274
[1350, 1550]	1437	1442	1447	1448	1444
[1550, 1850]	1678	1682	1676	1688	1681
[1850, 6500]	2255	2284	2259	2295	2273

Acknowledgements

We thank Christian Bierlich for his assistance with the Pythia prediction, and Klaus Werner and Mahbobeh Jafarpour for providing an EPOS release to generate $p\text{Ne}$ fixed-target collisions. We express our gratitude to our colleagues in the CERN accelerator departments for the excellent performance of the LHC. We thank the technical and administrative staff at the LHCb institutes. We express our gratitude to our colleagues in the CERN accelerator departments for the excellent performance of the LHC. We thank the technical and administrative staff at the LHCb institutes. We acknowledge support from CERN and from the national agencies: CAPES, CNPq, FAPERJ and FINEP (Brazil); MOST and NSFC (China); CNRS/IN2P3 (France); BMBF, DFG and MPG (Germany); INFN (Italy); NWO (Netherlands); MNiSW and NCN (Poland); MCID/IFA (Romania); MICIU and AEI (Spain); SNSF and SER (Switzerland); NASU (Ukraine); STFC (United Kingdom); DOE NP and NSF (USA). We acknowledge the computing resources that are provided by CERN, IN2P3 (France), KIT and DESY (Germany), INFN (Italy), SURF (Netherlands), PIC (Spain), GridPP (United Kingdom), CSCS

(Switzerland), IFIN-HH (Romania), CBPF (Brazil), and Polish WLCG (Poland). We are indebted to the communities behind the multiple open-source software packages on which we depend. Individual groups or members have received support from ARC and ARDC (Australia); Key Research Program of Frontier Sciences of CAS, CAS PIFI, CAS CCEPP, Fundamental Research Funds for the Central Universities, and Sci. & Tech. Program of Guangzhou (China); Minciencias (Colombia); EPLANET, Marie Skłodowska-Curie Actions, ERC and NextGenerationEU (European Union); A*MIDEX, ANR, IPhU and Labex P2IO, and Région Auvergne-Rhône-Alpes (France); AvH Foundation (Germany); ICSC (Italy); Severo Ochoa and María de Maeztu Units of Excellence, GVA, XuntaGal, GENCAT, InTalent-Inditex and Prog. Atracción Talento CM (Spain); SRC (Sweden); the Leverhulme Trust, the Royal Society and UKRI (United Kingdom).

References

- [1] E. V. Shuryak, *Quantum chromodynamics and the theory of superdense matter*, [Phys. Rept. **61** \(1980\) 71.](#)
- [2] STAR collaboration, J. Adams *et al.*, *Experimental and theoretical challenges in the search for the quark-gluon plasma: The STAR collaboration's critical assessment of the evidence from RHIC collisions*, [Nucl. Phys. **A757** \(2005\) 102,](#) [arXiv:nucl-ex/0501009.](#)
- [3] PHENIX collaboration, K. Adcox *et al.*, *Formation of dense partonic matter in relativistic nucleus-nucleus collisions at RHIC: Experimental evaluation by the PHENIX collaboration*, [Nucl. Phys. **A757** \(2005\) 184,](#) [arXiv:nucl-ex/0410003.](#)
- [4] ALICE collaboration, S. Acharya *et al.*, *The ALICE experiment: a journey through QCD*, [Eur. Phys. J. **C84** \(2024\) 813,](#) [arXiv:2211.04384.](#)
- [5] PHENIX collaboration, C. Aidala *et al.*, *Creation of quark-gluon plasma droplets with three distinct geometries*, [Nature Phys. **15** \(2019\) 214,](#) [arXiv:1805.02973.](#)
- [6] D. de Florian and R. Sassot, *Nuclear parton distributions at next to leading order*, [Phys. Rev. **D69** \(2004\) 074028,](#) [arXiv:hep-ph/0311227.](#)
- [7] K. J. Eskola, V. J. Kolhinen, and R. Vogt, *Obtaining the nuclear gluon distribution from heavy quark decays to lepton pairs in pA collisions*, [Nucl. Phys. **A696** \(2001\) 729,](#) [arXiv:hep-ph/0104124.](#)
- [8] T. Dai, J.-F. Paquet, D. Teaney, and S. A. Bass, *Parton energy loss in a hard-soft factorized approach*, [Phys. Rev. **C105** \(2022\) 034905,](#) [arXiv:2012.03441.](#)
- [9] A. Capella, A. Kaidalov, A. Kouider Akil, and C. Gerschel, *J/ψ and ψ' suppression in heavy ion collisions*, [Phys. Lett. **B393** \(1997\) 431,](#) [arXiv:hep-ph/9607265.](#)
- [10] A. Capella, E. G. Ferreira, and E. G. Ferreira, *J/ψ suppression and the decrease of nuclear absorption with increasing energy*, [Phys. Rev. **C76** \(2007\) 064906,](#) [arXiv:hep-ph/0610313.](#)

- [11] N. Armesto, *Small collision systems: theory overview on cold nuclear matter effects*, [EPJ Web Conf. **171** \(2018\) 11001](#).
- [12] J. Rafelski and B. Müller, *Strangeness production in the quark-gluon plasma*, [Phys. Rev. Lett. **48** \(1982\) 1066](#).
- [13] WA97 collaboration, E. Andersen *et al.*, *Strangeness enhancement at mid-rapidity in Pb-Pb collisions at 158 A GeV/c*, [Phys. Lett. **B449** \(1999\) 401](#).
- [14] STAR collaboration, B. I. Abelev *et al.*, *Enhanced strange baryon production in Au+Au collisions compared to p+p at $\sqrt{s_{NN}} = 200$ GeV*, [Phys. Rev. **C77** \(2008\) 044908](#), [arXiv:0705.2511](#).
- [15] ALICE collaboration, J. Adam *et al.*, *Enhanced production of multi-strange hadrons in high-multiplicity proton-proton collisions*, [Nature Phys. **13** \(2017\) 535](#), [arXiv:1606.07424](#).
- [16] S. Okubo, *ϕ meson and unitary symmetry model*, [Phys. Lett. **5** \(1963\) 165](#).
- [17] G. Zweig, *An SU_3 model for strong interaction symmetry and its breaking. Version 1*, doi: [10.17181/CERN-TH-401](#).
- [18] J. Iizuka, *Systematics and phenomenology of meson family*, [Prog. Theor. Phys. Suppl. **37** \(1966\) 21](#).
- [19] A. Shor, *ϕ -meson production as a probe of the quark-gluon plasma*, [Phys. Rev. Lett. **54** \(1985\) 1122](#).
- [20] N. Armesto, M. A. Braun, E. G. Ferreira, and C. Pajares, *Strangeness enhancement and string fusion in nucleus-nucleus collisions*, [Phys. Lett. **B344** \(1995\) 301](#).
- [21] J. R. Christiansen and P. Z. Skands, *String formation beyond leading colour*, [JHEP **08** \(2015\) 003](#), [arXiv:1505.01681](#).
- [22] C. Bierlich, S. Chakraborty, G. Gustafson, and L. Lönnblad, *Strangeness enhancement across collision systems without a plasma*, [Phys. Lett. **B835** \(2022\) 137571](#), [arXiv:2205.11170](#).
- [23] LHCb collaboration, A. A. Alves Jr. *et al.*, *The LHCb detector at the LHC*, [JINST **3** \(2008\) S08005](#).
- [24] LHCb collaboration, R. Aaij *et al.*, *LHCb detector performance*, [Int. J. Mod. Phys. **A30** \(2015\) 1530022](#), [arXiv:1412.6352](#).
- [25] LHCb collaboration, R. Aaij *et al.*, *Precision luminosity measurements at LHCb*, [JINST **9** \(2014\) P12005](#), [arXiv:1410.0149](#).
- [26] T. Sjöstrand, S. Mrenna, and P. Skands, *A brief introduction to PYTHIA 8.1*, [Comput. Phys. Commun. **178** \(2008\) 852](#), [arXiv:0710.3820](#).
- [27] I. Belyaev *et al.*, *Handling of the generation of primary events in Gauss, the LHCb simulation framework*, [J. Phys. Conf. Ser. **331** \(2011\) 032047](#).

- [28] T. Pierog *et al.*, *EPOS LHC: Test of collective hadronization with data measured at the CERN Large Hadron Collider*, *Phys. Rev.* **C92** (2015) 034906.
- [29] Geant4 collaboration, S. Agostinelli *et al.*, *Geant4: A simulation toolkit*, *Nucl. Instrum. Meth.* **A506** (2003) 250.
- [30] Geant4 collaboration, J. Allison *et al.*, *Geant4 developments and applications*, *IEEE Trans. Nucl. Sci.* **53** (2006) 270.
- [31] LHCb collaboration, M. Clemencic *et al.*, *The LHCb simulation application, Gauss: Design, evolution and experience*, *J. Phys. Conf. Ser.* **331** (2011) 032023.
- [32] R. Aaij *et al.*, *The LHCb trigger and its performance in 2011*, *JINST* **8** (2013) P04022, [arXiv:1211.3055](#).
- [33] Particle Data Group, S. Navas *et al.*, *Review of particle physics*, *Phys. Rev.* **D110** (2024) 030001.
- [34] T. Prohaska *et al.*, *Standard atomic weights of the elements 2021 (IUPAC technical report)*, *Pure and Applied Chemistry* **94** (2022) 573.
- [35] LHCb collaboration, R. Aaij *et al.*, *J/ψ and D^0 production in $\sqrt{s_{NN}} = 68.5$ GeV PbNe collisions*, *Eur. Phys. J.* **C83** (2023) 658, [arXiv:2211.11652](#).
- [36] LHCb collaboration, R. Aaij *et al.*, *Measurement of antiproton production in pHe collisions at $\sqrt{s_{NN}} = 110$ GeV*, *Phys. Rev. Lett.* **121** (2018) 222001, [arXiv:1808.06127](#).
- [37] LHCb collaboration, R. Aaij *et al.*, *Measurement of the track reconstruction efficiency at LHCb*, *JINST* **10** (2015) P02007, [arXiv:1408.1251](#).
- [38] LHCb collaboration, R. Aaij *et al.*, *Charmonium production in pNe collisions at $\sqrt{s_{NN}} = 68.5$ GeV*, *Eur. Phys. J.* **C83** (2023) 625, [arXiv:2211.11645](#).
- [39] C. Bierlich *et al.*, *A comprehensive guide to the physics and usage of PYTHIA 8.3*, *SciPost Phys. Codeb.* **8** (2022) , [arXiv:2203.11601](#).
- [40] K. Werner, *Revealing a deep connection between factorization and saturation: new insight into modeling high-energy proton-proton and nucleus-nucleus scattering in the EPOS4 framework*, *Phys. Rev.* **C108** (2023) 064903, [arXiv:2301.12517](#).
- [41] K. Werner and B. Guiot, *Perturbative QCD concerning light and heavy flavor in the EPOS4 framework*, *Phys. Rev.* **C108** (2023) 034904, [arXiv:2306.02396](#).
- [42] K. Werner, *Parallel scattering, saturation, and generalized Abramovskii-Gribov-Kancheli (AGK) theorem in the EPOS4 framework, with applications for heavy-ion collisions at $\sqrt{s_{NN}}$ of 5.02 TeV and 200 GeV*, *Phys. Rev.* **C109** (2024) 034918, [arXiv:2310.09380](#).
- [43] K. Werner, *Core-corona procedure and microcanonical hadronization to understand strangeness enhancement in proton-proton and heavy ion collisions in the EPOS4 framework*, *Phys. Rev.* **C109** (2024) 014910, [arXiv:2306.10277](#).
- [44] C. Bierlich, G. Gustafson, L. Lönnblad, and H. Shah, *The Angantyr model for heavy-ion collisions in PYTHIA8*, *JHEP* **10** (2018) 134, [arXiv:1806.10820](#).

LHCb collaboration

R. Aaij³⁸ , A.S.W. Abdelmotteleb⁵⁷ , C. Abellan Beteta⁵¹ , F. Abudinén⁵⁷ ,
 T. Ackernley⁶¹ , A. A. Adefisoye⁶⁹ , B. Adeva⁴⁷ , M. Adinolfi⁵⁵ , P. Adlarson⁸² ,
 C. Agapopoulou¹⁴ , C.A. Aidala⁸³ , Z. Ajaltouni¹¹ , S. Akar⁶⁶ , K. Akiba³⁸ ,
 P. Albicocco²⁸ , J. Albrecht^{19,f} , F. Alessio⁴⁹ , M. Alexander⁶⁰ , Z. Aliouche⁶³ ,
 P. Alvarez Cartelle⁵⁶ , R. Amalric¹⁶ , S. Amato³ , J.L. Amey⁵⁵ , Y. Amhis¹⁴ ,
 L. An⁶ , L. Anderlini²⁷ , M. Andersson⁵¹ , A. Andreianov⁴⁴ , P. Andreola⁵¹ ,
 M. Andreotti²⁶ , D. Andreou⁶⁹ , A. Anelli^{31,o} , D. Ao⁷ , F. Archilli^{37,u} ,
 M. Argenton²⁶ , S. Arguedas Cuendis^{9,49} , A. Artamonov⁴⁴ , M. Artuso⁶⁹ ,
 E. Aslanides¹³ , R. Ataíde Da Silva⁵⁰ , M. Atzeni⁶⁵ , B. Audurier¹² , D. Bacher⁶⁴ ,
 I. Bachiller Perea¹⁰ , S. Bachmann²² , M. Bachmayer⁵⁰ , J.J. Back⁵⁷ ,
 P. Baladron Rodriguez⁴⁷ , V. Balagura¹⁵ , A. Balboni²⁶ , W. Baldini²⁶ , L. Balzani¹⁹ ,
 H. Bao⁷ , J. Baptista de Souza Leite⁶¹ , C. Barbero Pretel^{47,12} , M. Barbetti²⁷ , I.
 R. Barbosa⁷⁰ , R.J. Barlow⁶³ , M. Barnyakov²⁵ , S. Barsuk¹⁴ , W. Barter⁵⁹ ,
 M. Bartolini⁵⁶ , J. Bartz⁶⁹ , J.M. Basels¹⁷ , S. Bashir⁴⁰ , G. Bassi^{35,r} , B. Batsukh⁵ ,
 P. B. Battista¹⁴ , A. Bay⁵⁰ , A. Beck⁵⁷ , M. Becker¹⁹ , F. Bedeschi³⁵ , I.B. Bediaga² ,
 N. A. Behling¹⁹ , S. Belin⁴⁷ , K. Belous⁴⁴ , I. Belov²⁹ , I. Belyaev³⁶ , G. Benane¹³ ,
 G. Bencivenni²⁸ , E. Ben-Haim¹⁶ , A. Berezhnoy⁴⁴ , R. Bernet⁵¹ , S. Bernet Andres⁴⁵ ,
 A. Bertolin³³ , C. Betancourt⁵¹ , F. Betti⁵⁹ , J. Bex⁵⁶ , Ia. Bezshyiko⁵¹ , J. Bhom⁴¹ ,
 M.S. Bieker¹⁹ , N.V. Biesuz²⁶ , P. Billoir¹⁶ , A. Biolchini³⁸ , M. Birch⁶² ,
 F.C.R. Bishop¹⁰ , A. Bitadze⁶³ , A. Bizzeti , T. Blake⁵⁷ , F. Blanc⁵⁰ , J.E. Blank¹⁹ ,
 S. Blusk⁶⁹ , V. Bocharnikov⁴⁴ , J.A. Boelhaue¹⁹ , O. Boente Garcia¹⁵ ,
 T. Boettcher⁶⁶ , A. Bohare⁵⁹ , A. Boldyrev⁴⁴ , C.S. Bolognani⁷⁹ , R. Bolzonella^{26,l} , R.
 B. Bonacci¹ , N. Bondar⁴⁴ , A. Bordelius⁴⁹ , F. Borgato^{33,p} , S. Borghi⁶³ ,
 M. Borsato^{31,o} , J.T. Borsuk⁴¹ , S.A. Bouchiba⁵⁰ , M. Bovill⁶⁴ , T.J.V. Bowcock⁶¹ ,
 A. Boyer⁴⁹ , C. Bozzi²⁶ , A. Brea Rodriguez⁵⁰ , N. Breer¹⁹ , J. Brodzicka⁴¹ ,
 A. Brossa Gonzalo^{47,†} , J. Brown⁶¹ , D. Brundu³² , E. Buchanan⁵⁹ , A. Buonauro⁵¹ ,
 L. Buonincontri^{33,p} , A.T. Burke⁶³ , C. Burr⁴⁹ , J.S. Butter⁵⁶ , J. Buytaert⁴⁹ ,
 W. Byczynski⁴⁹ , S. Cadeddu³² , H. Cai⁷⁴ , A. C. Caillet¹⁶ , R. Calabrese^{26,l} ,
 S. Calderon Ramirez⁹ , L. Calefice⁴⁶ , S. Cali²⁸ , M. Calvi^{31,o} , M. Calvo Gomez⁴⁵ ,
 P. Camargo Magalhaes^{2,y} , J. I. Cambon Bouzas⁴⁷ , P. Campana²⁸ ,
 D.H. Campora Perez⁷⁹ , A.F. Campoverde Quezada⁷ , S. Capelli³¹ , L. Capriotti²⁶ ,
 R. Caravaca-Mora⁹ , A. Carbone^{25,j} , L. Carcedo Salgado⁴⁷ , R. Cardinale^{29,m} ,
 A. Cardini³² , P. Carniti^{31,o} , L. Carus²² , A. Casais Vidal⁶⁵ , R. Caspary²² ,
 G. Casse⁶¹ , M. Cattaneo⁴⁹ , G. Cavallero^{26,49} , V. Cavallini^{26,l} , S. Celani²² ,
 D. Cervenkov⁶⁴ , S. Cesare^{30,n} , A.J. Chadwick⁶¹ , I. Chahrour⁸³ , M. Charles¹⁶ ,
 Ph. Charpentier⁴⁹ , E. Chatzianagnostou³⁸ , M. Chefdeville¹⁰ , C. Chen¹³ , S. Chen⁵ ,
 Z. Chen⁷ , A. Chernov⁴¹ , S. Chernyshenko⁵³ , X. Chiotopoulos⁷⁹ , V. Chobanova⁸¹ ,
 S. Cholak⁵⁰ , M. Chrzaszcz⁴¹ , A. Chubykin⁴⁴ , V. Chulikov²⁸ , P. Ciambrone²⁸ ,
 X. Cid Vidal⁴⁷ , G. Ciezarek⁴⁹ , P. Cifra⁴⁹ , P.E.L. Clarke⁵⁹ , M. Clemencic⁴⁹ ,
 H.V. Cliff⁵⁶ , J. Closier⁴⁹ , C. Cocha Toapaxi²² , V. Coco⁴⁹ , J. Cogan¹³ ,
 E. Cogneras¹¹ , L. Cojocariu⁴³ , S. Collaviti⁵⁰ , P. Collins⁴⁹ , T. Colombo⁴⁹ , M. C.
 Colonna¹⁹ , A. Comerma-Montells⁴⁶ , L. Congedo²⁴ , A. Contu³² , N. Cooke⁶⁰ ,
 I. Corredoira⁴⁷ , A. Correia¹⁶ , G. Corti⁴⁹ , J.J. Cottee Meldrum⁵⁵ , B. Couturier⁴⁹ ,
 D.C. Craik⁵¹ , M. Cruz Torres^{2,g} , E. Curras Rivera⁵⁰ , R. Currie⁵⁹ , C.L. Da Silva⁶⁸ ,
 S. Dadabaev⁴⁴ , L. Dai⁷¹ , X. Dai⁶ , E. Dall'Occo⁴⁹ , J. Dalseno⁴⁷ ,
 C. D'Ambrosio⁴⁹ , J. Daniel¹¹ , A. Danilina⁴⁴ , P. d'Argent²⁴ , G. Darze³ , A.
 Davidson⁵⁷ , J.E. Davies⁶³ , A. Davis⁶³ , O. De Aguiar Francisco⁶³ , C. De Angelis^{32,k} ,
 F. De Benedetti⁴⁹ , J. de Boer³⁸ , K. De Bruyn⁷⁸ , S. De Capua⁶³ , M. De Cian²² ,

D. Karpenkov⁴⁴, A. Kauniskangas⁵⁰, J.W. Kautz⁶⁶, M.K. Kazanecki⁴¹, F. Keizer⁴⁹, M. Kenzie⁵⁶, T. Ketel³⁸, B. Khanji⁶⁹, A. Kharisova⁴⁴, S. Kholodenko^{35,49}, G. Khreich¹⁴, T. Kirn¹⁷, V.S. Kirsebom^{31,o}, O. Kitouni⁶⁵, S. Klaver³⁹, N. Kleijne^{35,r}, K. Klimaszewski⁴², M.R. Kmiec⁴², S. Koliiev⁵³, L. Kolk¹⁹, A. Konoplyannikov⁴⁴, P. Kopiciewicz^{40,49}, P. Koppenburg³⁸, M. Korolev⁴⁴, I. Kostiuk³⁸, O. Kot⁵³, S. Kotriakhova, A. Kozachuk⁴⁴, P. Kravchenko⁴⁴, L. Kravchuk⁴⁴, M. Kreps⁵⁷, P. Krokovny⁴⁴, W. Krupa⁶⁹, W. Krzemien⁴², O. Kshyvanskiy⁵³, S. Kubis⁸⁰, M. Kucharczyk⁴¹, V. Kudryavtsev⁴⁴, E. Kulikova⁴⁴, A. Kupsc⁸², B. K. Kutsenko¹³, D. Lacarrere⁴⁹, P. Laguarda Gonzalez⁴⁶, A. Lai³², A. Lampis³², D. Lancierini⁵⁶, C. Landesa Gomez⁴⁷, J.J. Lane¹, R. Lane⁵⁵, G. Lanfranchi²⁸, C. Langenbruch²², J. Langer¹⁹, O. Lantwin⁴⁴, T. Latham⁵⁷, F. Lazzari^{35,s}, C. Lazzeroni⁵⁴, R. Le Gac¹³, H. Lee⁶¹, R. Lefèvre¹¹, A. Leflat⁴⁴, S. Legotin⁴⁴, M. Lehuraux⁵⁷, E. Lemos Cid⁴⁹, O. Leroy¹³, T. Lesiak⁴¹, E. D. Lesser⁴⁹, B. Leverington²², A. Li^{4,b}, C. Li¹³, H. Li⁷², K. Li⁸, L. Li⁶³, M. Li⁸, P. Li⁷, P.-R. Li⁷³, Q. Li^{5,7}, S. Li⁸, T. Li^{5,d}, T. Li⁷², Y. Li⁸, Y. Li⁵, Z. Lian^{4,b}, X. Liang⁶⁹, S. Libralon⁴⁸, C. Lin⁷, T. Lin⁵⁸, R. Lindner⁴⁹, H. Linton⁶², V. Lisovskyi⁵⁰, R. Litvinov^{32,49}, F. L. Liu¹, G. Liu⁷², K. Liu⁷³, S. Liu^{5,7}, W. Liu⁸, Y. Liu⁵⁹, Y. Liu⁷³, Y. L. Liu⁶², A. Lobo Salvia⁴⁶, A. Loi³², T. Long⁵⁶, J.H. Lopes³, A. Lopez Huertas⁴⁶, S. López Soliño⁴⁷, Q. Lu¹⁵, C. Lucarelli²⁷, D. Lucchesi^{33,p}, M. Lucio Martinez⁷⁹, V. Lukashenko^{38,53}, Y. Luo⁶, A. Lupato^{33,i}, E. Luppi^{26,l}, K. Lynch²³, X.-R. Lyu⁷, G. M. Ma^{4,b}, S. Maccolini¹⁹, F. Machefert¹⁴, F. Maciuc⁴³, B. Mack⁶⁹, I. Mackay⁶⁴, L. M. Mackey⁶⁹, L.R. Madhan Mohan⁵⁶, M. J. Madurai⁵⁴, A. Maevskiy⁴⁴, D. Magdalinski³⁸, D. Maisuzenko⁴⁴, M.W. Majewski⁴⁰, J.J. Malczewski⁴¹, S. Malde⁶⁴, L. Malentacca⁴⁹, A. Malinin⁴⁴, T. Maltsev⁴⁴, G. Manca^{32,k}, G. Mancinelli¹³, C. Mancuso^{30,14,n}, R. Manera Escalero⁴⁶, F. M. Mangarella³⁷, D. Manuzzi²⁵, D. Marangotto^{30,n}, J.F. Marchand¹⁰, R. Marchevski⁵⁰, U. Marconi²⁵, E. Mariani¹⁶, S. Mariani⁴⁹, C. Marin Benito^{46,49}, J. Marks²², A.M. Marshall⁵⁵, L. Martel⁶⁴, G. Martelli^{34,q}, G. Martellotti³⁶, L. Martinazzoli⁴⁹, M. Martinelli^{31,o}, D. Martinez Gomez⁷⁸, D. Martinez Santos⁸¹, F. Martinez Vidal⁴⁸, A. Martorell i Granollers⁴⁵, A. Massafferri², R. Matev⁴⁹, A. Mathad⁴⁹, V. Matiunin⁴⁴, C. Matteuzzi⁶⁹, K.R. Mattioli¹⁵, A. Mauri⁶², E. Maurice¹⁵, J. Mauricio⁴⁶, P. Mayencourt⁵⁰, J. Mazorra de Cos⁴⁸, M. Mazurek⁴², M. McCann⁶², L. McConnell²³, T.H. McGrath⁶³, N.T. McHugh⁶⁰, A. McNab⁶³, R. McNulty²³, B. Meadows⁶⁶, G. Meier¹⁹, D. Melnychuk⁴², F. M. Meng^{4,b}, M. Merk^{38,79}, A. Merli⁵⁰, L. Meyer Garcia⁶⁷, D. Miao^{5,7}, H. Miao⁷, M. Mikhasenko⁷⁶, D.A. Milanes⁷⁵, A. Minotti^{31,o}, E. Minucci²⁸, T. Miralles¹¹, B. Mitreska¹⁹, D.S. Mitzel¹⁹, A. Modak⁵⁸, R.A. Mohammed⁶⁴, R.D. Moise¹⁷, S. Mokhenko⁴⁴, E. F. Molina Cardenas⁸³, T. Mombächer⁴⁹, M. Monk^{57,1}, S. Monteil¹¹, A. Morcillo Gomez⁴⁷, G. Morello²⁸, M.J. Morello^{35,r}, M.P. Morgenthaler²², J. Moron⁴⁰, W. Morren³⁸, A.B. Morris⁴⁹, A.G. Morris¹³, R. Mountain⁶⁹, H. Mu^{4,b}, Z. M. Mu⁶, E. Muhammad⁵⁷, F. Muheim⁵⁹, M. Mulder⁷⁸, K. Müller⁵¹, F. Muñoz-Rojas⁹, R. Murta⁶², P. Naik⁶¹, T. Nakada⁵⁰, R. Nandakumar⁵⁸, T. Nanut⁴⁹, I. Nasteva³, M. Needham⁵⁹, N. Neri^{30,n}, S. Neubert¹⁸, N. Neufeld⁴⁹, P. Neustroev⁴⁴, J. Nicolini^{19,14}, D. Nicotra⁷⁹, E.M. Niel⁴⁹, N. Nikitin⁴⁴, Q. Niu⁷³, P. Nogaroli³, P. Nogga¹⁸, C. Normand⁵⁵, J. Novoa Fernandez⁴⁷, G. Nowak⁶⁶, C. Nunez⁸³, H. N. Nur⁶⁰, A. Oblakowska-Mucha⁴⁰, V. Obraztsov⁴⁴, T. Oeser¹⁷, S. Okamura^{26,l}, A. Okhotnikov⁴⁴, O. Okhrimenko⁵³, R. Oldeman^{32,k}, F. Oliva⁵⁹, M. Olocco¹⁹, C.J.G. Onderwater⁷⁹, R.H. O'Neil⁵⁹, D. Osthues¹⁹, J.M. Otalora Goicochea³, P. Owen⁵¹, A. Oyanguren⁴⁸, O. Ozcelik⁵⁹, F. Paciolla^{35,v},

A. Padee⁴² , K.O. Padeken¹⁸ , B. Pagare⁵⁷ , P.R. Pais²² , T. Pajero⁴⁹ , A. Palano²⁴ ,
 M. Palutan²⁸ , X. Pan^{4,b} , G. Panshin⁴⁴ , L. Paolucci⁵⁷ , A. Papanestis^{58,49} ,
 M. Pappagallo^{24,h} , L.L. Pappalardo^{26,l} , C. Pappenheimer⁶⁶ , C. Parkes⁶³ , D.
 Parmar⁷⁶ , B. Passalacqua^{26,l} , G. Passaleva²⁷ , D. Passaro^{35,r} , A. Pastore²⁴ ,
 M. Patel⁶² , J. Patoc⁶⁴ , C. Patrignani^{25,j} , A. Paul⁶⁹ , C.J. Pawley⁷⁹ ,
 A. Pellegrino³⁸ , J. Peng^{5,7} , M. Pepe Altarelli²⁸ , S. Perazzini²⁵ , D. Pereima⁴⁴ , H.
 Pereira Da Costa⁶⁸ , A. Pereiro Castro⁴⁷ , P. Perret¹¹ , A. Perrevoort⁷⁸ , A. Perro⁴⁹ ,
 M.J. Peters⁶⁶ , K. Petridis⁵⁵ , A. Petrolini^{29,m} , J. P. Pfaller⁶⁶ , H. Pham⁶⁹ ,
 L. Pica^{35,r} , M. Piccini³⁴ , L. Piccolo³² , B. Pietrzyk¹⁰ , G. Pietrzyk¹⁴ , D. Pinci³⁶ ,
 F. Pisani⁴⁹ , M. Pizzichemi^{31,o,49} , V. Placinta⁴³ , M. Plo Casaus⁴⁷ , T. Poeschl⁴⁹ ,
 F. Polci^{16,49} , M. Poli Lener²⁸ , A. Poluektov¹³ , N. Polukhina⁴⁴ , I. Polyakov⁴⁴ ,
 E. Polycarpo³ , S. Ponce⁴⁹ , D. Popov⁷ , S. Poslavskii⁴⁴ , K. Prasanth⁵⁹ ,
 C. Prouve⁸¹ , D. Provenzano^{32,k} , V. Pugatch⁵³ , G. Punzi^{35,s} , S. Qasim⁵¹ , Q. Q.
 Qian⁶ , W. Qian⁷ , N. Qin^{4,b} , S. Qu^{4,b} , R. Quagliani⁴⁹ , R.I. Rabadan Trejo⁵⁷ ,
 J.H. Rademacker⁵⁵ , M. Rama³⁵ , M. Ramírez García⁸³ , V. Ramos De Oliveira⁷⁰ ,
 M. Ramos Pernas⁵⁷ , M.S. Rangel³ , F. Ratnikov⁴⁴ , G. Raven³⁹ ,
 M. Rebollo De Miguel⁴⁸ , F. Redi^{30,i} , J. Reich⁵⁵ , F. Reiss⁶³ , Z. Ren⁷ ,
 P.K. Resmi⁶⁴ , R. Ribatti⁵⁰ , G. R. Ricart^{15,12} , D. Riccardi^{35,r} , S. Ricciardi⁵⁸ ,
 K. Richardson⁶⁵ , M. Richardson-Slipper⁵⁹ , K. Rinnert⁶¹ , P. Robbe^{14,49} ,
 G. Robertson⁶⁰ , E. Rodrigues⁶¹ , A. Rodriguez Alvarez⁴⁶ , E. Rodriguez Fernandez⁴⁷ ,
 J.A. Rodriguez Lopez⁷⁵ , E. Rodriguez Rodriguez⁴⁷ , J. Roensch¹⁹ , A. Rogachev⁴⁴ ,
 A. Rogovskiy⁵⁸ , D.L. Rolf⁴⁹ , P. Roloff⁴⁹ , V. Romanovskiy⁶⁶ , A. Romero Vidal⁴⁷ ,
 G. Romolini²⁶ , F. Ronchetti⁵⁰ , T. Rong⁶ , M. Rotondo²⁸ , S. R. Roy²² ,
 M.S. Rudolph⁶⁹ , M. Ruiz Diaz²² , R.A. Ruiz Fernandez⁴⁷ , J. Ruiz Vidal^{82,z} ,
 A. Ryzhikov⁴⁴ , J. Ryzka⁴⁰ , J. J. Saavedra-Arias⁹ , J.J. Saborido Silva⁴⁷ , R. Sadek¹⁵ ,
 N. Sagidova⁴⁴ , D. Sahoo⁷⁷ , N. Sahoo⁵⁴ , B. Saitta^{32,k} , M. Salomoni^{31,49,o} ,
 I. Sanderswood⁴⁸ , R. Santacesaria³⁶ , C. Santamarina Rios⁴⁷ , M. Santimaria^{28,49} ,
 L. Santoro² , E. Santovetti³⁷ , A. Saputi^{26,49} , D. Saranin⁴⁴ , A. Sarnatskiy⁷⁸ ,
 G. Sarpis⁵⁹ , M. Sarpis⁶³ , C. Satriano^{36,t} , A. Satta³⁷ , M. Saur⁶ , D. Savrina⁴⁴ ,
 H. Sazak¹⁷ , F. Sborzacchi^{49,28} , L.G. Scantlebury Smead⁶⁴ , A. Scarabotto¹⁹ ,
 S. Schael¹⁷ , S. Scherl⁶¹ , M. Schiller⁶⁰ , H. Schindler⁴⁹ , M. Schmelling²¹ ,
 B. Schmidt⁴⁹ , S. Schmitt¹⁷ , H. Schmitz¹⁸ , O. Schneider⁵⁰ , A. Schopper⁴⁹ ,
 N. Schulte¹⁹ , S. Schulte⁵⁰ , M.H. Schune¹⁴ , R. Schwemmer⁴⁹ , G. Schwering¹⁷ ,
 B. Sciascia²⁸ , A. Sciuccati⁴⁹ , I. Segal⁷⁶ , S. Sellam⁴⁷ , A. Semennikov⁴⁴ ,
 T. Senger⁵¹ , M. Senghi Soares³⁹ , A. Sergi^{29,m} , N. Serra⁵¹ , L. Sestini³³ ,
 A. Seuthe¹⁹ , Y. Shang⁶ , D.M. Shangase⁸³ , M. Shapkin⁴⁴ , R. S. Sharma⁶⁹ ,
 I. Shchemerov⁴⁴ , L. Shchutka⁵⁰ , T. Shears⁶¹ , L. Shekhtman⁴⁴ , Z. Shen⁶ ,
 S. Sheng^{5,7} , V. Shevchenko⁴⁴ , B. Shi⁷ , Q. Shi⁷ , Y. Shimizu¹⁴ , E. Shmanin²⁵ ,
 R. Shorkin⁴⁴ , J.D. Shupperd⁶⁹ , R. Silva Coutinho⁶⁹ , G. Simi^{33,p} , S. Simone^{24,h} ,
 N. Skidmore⁵⁷ , T. Skwarnicki⁶⁹ , M.W. Slater⁵⁴ , J.C. Smallwood⁶⁴ , E. Smith⁶⁵ ,
 K. Smith⁶⁸ , M. Smith⁶² , A. Snoch³⁸ , L. Soares Lavra⁵⁹ , M.D. Sokoloff⁶⁶ ,
 F.J.P. Soler⁶⁰ , A. Solomin^{44,55} , A. Solovev⁴⁴ , I. Solovyev⁴⁴ , N. S. Sommerfeld¹⁸ ,
 R. Song¹ , Y. Song⁵⁰ , Y. Song^{4,b} , Y. S. Song⁶ , F.L. Souza De Almeida⁶⁹ ,
 B. Souza De Paula³ , E. Spadaro Norella^{29,m} , E. Spedicato²⁵ , J.G. Speer¹⁹ ,
 E. Spiridenkov⁴⁴ , P. Spradlin⁶⁰ , V. Sriskaran⁴⁹ , F. Stagni⁴⁹ , M. Stahl⁴⁹ , S. Stahl⁴⁹ ,
 S. Stanislaus⁶⁴ , E.N. Stein⁴⁹ , O. Steinkamp⁵¹ , O. Stenyakin⁴⁴ , H. Stevens¹⁹ ,
 D. Strelalina⁴⁴ , Y. Su⁷ , F. Suljik⁶⁴ , J. Sun³² , L. Sun⁷⁴ , D. Sundfeld² ,
 W. Sutcliffe⁵¹ , P.N. Swallow⁵⁴ , K. Swientek⁴⁰ , F. Swystun⁵⁶ , A. Szabelski⁴² ,
 T. Szumlak⁴⁰ , Y. Tan^{4,b} , Y. Tang⁷⁴ , M.D. Tat⁶⁴ , A. Terentev⁴⁴ ,
 F. Terzuoli^{35,v,49} , F. Teubert⁴⁹ , E. Thomas⁴⁹ , D.J.D. Thompson⁵⁴ , H. Tilquin⁶² ,

V. Tisserand¹¹ , S. T’Jampens¹⁰ , M. Tobin^{5,49} , L. Tomassetti^{26,l} , G. Tonani^{30,n,49} , X. Tong⁶ , D. Torres Machado² , L. Toscano¹⁹ , D.Y. Tou^{4,b} , C. Tripl⁴⁵ , G. Tuci²² , N. Tuning³⁸ , L.H. Uecker²² , A. Ukleja⁴⁰ , D.J. Unverzagt²² , B. Urbach⁵⁹ , E. Ursov⁴⁴ , A. Usachov³⁹ , A. Ustyuzhanin⁴⁴ , U. Uwer²² , V. Vagnoni²⁵ , V. Valcarce Cadenas⁴⁷ , G. Valenti²⁵ , N. Valls Canudas⁴⁹ , H. Van Hecke⁶⁸ , E. van Herwijnen⁶² , C.B. Van Hulse^{47,x} , R. Van Laak⁵⁰ , M. van Veghel³⁸ , G. Vasquez⁵¹ , R. Vazquez Gomez⁴⁶ , P. Vazquez Regueiro⁴⁷ , C. Vázquez Sierra⁴⁷ , S. Vecchi²⁶ , J.J. Velthuis⁵⁵ , M. Veltri^{27,w} , A. Venkateswaran⁵⁰ , M. Verdoggia³² , M. Vesterinen⁵⁷ , D. Vico Benet⁶⁴ , P. Vidrier Villalba⁴⁶ , M. Vieites Diaz⁴⁹ , X. Vilasis-Cardona⁴⁵ , E. Vilella Figueras⁶¹ , A. Villa²⁵ , P. Vincent¹⁶ , F.C. Volle⁵⁴ , D. vom Bruch¹³ , N. Voropaev⁴⁴ , K. Vos⁷⁹ , C. Vrahas⁵⁹ , J. Wagner¹⁹ , J. Walsh³⁵ , E.J. Walton^{1,57} , G. Wan⁶ , C. Wang²² , G. Wang⁸ , H. Wang⁷³ , J. Wang⁶ , J. Wang⁵ , J. Wang^{4,b} , J. Wang⁷⁴ , M. Wang³⁰ , N. W. Wang⁷ , R. Wang⁵⁵ , X. Wang⁸ , X. Wang⁷² , X. W. Wang⁶² , Y. Wang⁶ , Y. W. Wang⁷³ , Z. Wang¹⁴ , Z. Wang^{4,b} , Z. Wang³⁰ , J.A. Ward^{57,1} , M. Waterlaet⁴⁹ , N.K. Watson⁵⁴ , D. Websdale⁶² , Y. Wei⁶ , J. Wendel⁸¹ , B.D.C. Westhenry⁵⁵ , C. White⁵⁶ , M. Whitehead⁶⁰ , E. Whiter⁵⁴ , A.R. Wiederhold⁶³ , D. Wiedner¹⁹ , G. Wilkinson⁶⁴ , M.K. Wilkinson⁶⁶ , M. Williams⁶⁵ , M. J. Williams⁴⁹ , M.R.J. Williams⁵⁹ , R. Williams⁵⁶ , Z. Williams⁵⁵ , F.F. Wilson⁵⁸ , M. Winn¹² , W. Wislicki⁴² , M. Witek⁴¹ , L. Witola²² , G. Wormser¹⁴ , S.A. Wotton⁵⁶ , H. Wu⁶⁹ , J. Wu⁸ , X. Wu⁷⁴ , Y. Wu⁶ , Z. Wu⁷ , K. Wyllie⁴⁹ , S. Xian⁷² , Z. Xiang⁵ , Y. Xie⁸ , A. Xu³⁵ , J. Xu⁷ , L. Xu^{4,b} , L. Xu^{4,b} , M. Xu⁵⁷ , Z. Xu⁴⁹ , Z. Xu⁷ , Z. Xu⁵ , K. Yang⁶² , S. Yang⁷ , X. Yang⁶ , Y. Yang^{29,m} , Z. Yang⁶ , V. Yeroshenko¹⁴ , H. Yeung⁶³ , H. Yin⁸ , X. Yin⁷ , C. Y. Yu⁶ , J. Yu⁷¹ , X. Yuan⁵ , Y. Yuan^{5,7} , E. Zaffaroni⁵⁰ , M. Zavertyaev²¹ , M. Zdybal⁴¹ , F. Zenesini^{25,j} , C. Zeng^{5,7} , M. Zeng^{4,b} , C. Zhang⁶ , D. Zhang⁸ , J. Zhang⁷ , L. Zhang^{4,b} , S. Zhang⁷¹ , S. Zhang⁶⁴ , Y. Zhang⁶ , Y. Z. Zhang^{4,b} , Y. Zhao²² , A. Zharkova⁴⁴ , A. Zhelezov²² , S. Z. Zheng⁶ , X. Z. Zheng^{4,b} , Y. Zheng⁷ , T. Zhou⁶ , X. Zhou⁸ , Y. Zhou⁷ , V. Zhovkovska⁵⁷ , L. Z. Zhu⁷ , X. Zhu^{4,b} , X. Zhu⁸ , V. Zhukov¹⁷ , J. Zhuo⁴⁸ , Q. Zou^{5,7} , D. Zuliani^{33,p} , G. Zunica⁵⁰ .

¹*School of Physics and Astronomy, Monash University, Melbourne, Australia*

²*Centro Brasileiro de Pesquisas Físicas (CBPF), Rio de Janeiro, Brazil*

³*Universidade Federal do Rio de Janeiro (UFRJ), Rio de Janeiro, Brazil*

⁴*Department of Engineering Physics, Tsinghua University, Beijing, China*

⁵*Institute Of High Energy Physics (IHEP), Beijing, China*

⁶*School of Physics State Key Laboratory of Nuclear Physics and Technology, Peking University, Beijing, China*

⁷*University of Chinese Academy of Sciences, Beijing, China*

⁸*Institute of Particle Physics, Central China Normal University, Wuhan, Hubei, China*

⁹*Consejo Nacional de Rectores (CONARE), San Jose, Costa Rica*

¹⁰*Université Savoie Mont Blanc, CNRS, IN2P3-LAPP, Annecy, France*

¹¹*Université Clermont Auvergne, CNRS/IN2P3, LPC, Clermont-Ferrand, France*

¹²*Université Paris-Saclay, Centre d’Etudes de Saclay (CEA), IRFU, Saclay, France, Gif-Sur-Yvette, France*

¹³*Aix Marseille Univ, CNRS/IN2P3, CPPM, Marseille, France*

¹⁴*Université Paris-Saclay, CNRS/IN2P3, IJCLab, Orsay, France*

¹⁵*Laboratoire Leprince-Ringuet, CNRS/IN2P3, Ecole Polytechnique, Institut Polytechnique de Paris, Palaiseau, France*

¹⁶*LPNHE, Sorbonne Université, Paris Diderot Sorbonne Paris Cité, CNRS/IN2P3, Paris, France*

¹⁷*I. Physikalisches Institut, RWTH Aachen University, Aachen, Germany*

¹⁸*Universität Bonn - Helmholtz-Institut für Strahlen und Kernphysik, Bonn, Germany*

¹⁹*Fakultät Physik, Technische Universität Dortmund, Dortmund, Germany*

- ²⁰ *Physikalisches Institut, Albert-Ludwigs-Universität Freiburg, Freiburg, Germany*
- ²¹ *Max-Planck-Institut für Kernphysik (MPIK), Heidelberg, Germany*
- ²² *Physikalisches Institut, Ruprecht-Karls-Universität Heidelberg, Heidelberg, Germany*
- ²³ *School of Physics, University College Dublin, Dublin, Ireland*
- ²⁴ *INFN Sezione di Bari, Bari, Italy*
- ²⁵ *INFN Sezione di Bologna, Bologna, Italy*
- ²⁶ *INFN Sezione di Ferrara, Ferrara, Italy*
- ²⁷ *INFN Sezione di Firenze, Firenze, Italy*
- ²⁸ *INFN Laboratori Nazionali di Frascati, Frascati, Italy*
- ²⁹ *INFN Sezione di Genova, Genova, Italy*
- ³⁰ *INFN Sezione di Milano, Milano, Italy*
- ³¹ *INFN Sezione di Milano-Bicocca, Milano, Italy*
- ³² *INFN Sezione di Cagliari, Monserrato, Italy*
- ³³ *INFN Sezione di Padova, Padova, Italy*
- ³⁴ *INFN Sezione di Perugia, Perugia, Italy*
- ³⁵ *INFN Sezione di Pisa, Pisa, Italy*
- ³⁶ *INFN Sezione di Roma La Sapienza, Roma, Italy*
- ³⁷ *INFN Sezione di Roma Tor Vergata, Roma, Italy*
- ³⁸ *Nikhef National Institute for Subatomic Physics, Amsterdam, Netherlands*
- ³⁹ *Nikhef National Institute for Subatomic Physics and VU University Amsterdam, Amsterdam, Netherlands*
- ⁴⁰ *AGH - University of Krakow, Faculty of Physics and Applied Computer Science, Kraków, Poland*
- ⁴¹ *Henryk Niewodniczanski Institute of Nuclear Physics Polish Academy of Sciences, Kraków, Poland*
- ⁴² *National Center for Nuclear Research (NCBJ), Warsaw, Poland*
- ⁴³ *Horia Hulubei National Institute of Physics and Nuclear Engineering, Bucharest-Magurele, Romania*
- ⁴⁴ *Affiliated with an institute covered by a cooperation agreement with CERN*
- ⁴⁵ *DS4DS, La Salle, Universitat Ramon Llull, Barcelona, Spain*
- ⁴⁶ *ICCUB, Universitat de Barcelona, Barcelona, Spain*
- ⁴⁷ *Instituto Galego de Física de Altas Enerxías (IGFAE), Universidade de Santiago de Compostela, Santiago de Compostela, Spain*
- ⁴⁸ *Instituto de Física Corpuscular, Centro Mixto Universidad de Valencia - CSIC, Valencia, Spain*
- ⁴⁹ *European Organization for Nuclear Research (CERN), Geneva, Switzerland*
- ⁵⁰ *Institute of Physics, Ecole Polytechnique Fédérale de Lausanne (EPFL), Lausanne, Switzerland*
- ⁵¹ *Physik-Institut, Universität Zürich, Zürich, Switzerland*
- ⁵² *NSC Kharkiv Institute of Physics and Technology (NSC KIPT), Kharkiv, Ukraine*
- ⁵³ *Institute for Nuclear Research of the National Academy of Sciences (KINR), Kyiv, Ukraine*
- ⁵⁴ *School of Physics and Astronomy, University of Birmingham, Birmingham, United Kingdom*
- ⁵⁵ *H.H. Wills Physics Laboratory, University of Bristol, Bristol, United Kingdom*
- ⁵⁶ *Cavendish Laboratory, University of Cambridge, Cambridge, United Kingdom*
- ⁵⁷ *Department of Physics, University of Warwick, Coventry, United Kingdom*
- ⁵⁸ *STFC Rutherford Appleton Laboratory, Didcot, United Kingdom*
- ⁵⁹ *School of Physics and Astronomy, University of Edinburgh, Edinburgh, United Kingdom*
- ⁶⁰ *School of Physics and Astronomy, University of Glasgow, Glasgow, United Kingdom*
- ⁶¹ *Oliver Lodge Laboratory, University of Liverpool, Liverpool, United Kingdom*
- ⁶² *Imperial College London, London, United Kingdom*
- ⁶³ *Department of Physics and Astronomy, University of Manchester, Manchester, United Kingdom*
- ⁶⁴ *Department of Physics, University of Oxford, Oxford, United Kingdom*
- ⁶⁵ *Massachusetts Institute of Technology, Cambridge, MA, United States*
- ⁶⁶ *University of Cincinnati, Cincinnati, OH, United States*
- ⁶⁷ *University of Maryland, College Park, MD, United States*
- ⁶⁸ *Los Alamos National Laboratory (LANL), Los Alamos, NM, United States*
- ⁶⁹ *Syracuse University, Syracuse, NY, United States*
- ⁷⁰ *Pontifícia Universidade Católica do Rio de Janeiro (PUC-Rio), Rio de Janeiro, Brazil, associated to ³*
- ⁷¹ *School of Physics and Electronics, Hunan University, Changsha City, China, associated to ⁸*
- ⁷² *Guangdong Provincial Key Laboratory of Nuclear Science, Guangdong-Hong Kong Joint Laboratory of Quantum Matter, Institute of Quantum Matter, South China Normal University, Guangzhou, China,*

associated to ⁴

⁷³ Lanzhou University, Lanzhou, China, associated to ⁵

⁷⁴ School of Physics and Technology, Wuhan University, Wuhan, China, associated to ⁴

⁷⁵ Departamento de Física , Universidad Nacional de Colombia, Bogota, Colombia, associated to ¹⁶

⁷⁶ Ruhr Universitaet Bochum, Fakultaet f. Physik und Astronomie, Bochum, Germany, associated to ¹⁹

⁷⁷ Eotvos Lorand University, Budapest, Hungary, associated to ⁴⁹

⁷⁸ Van Swinderen Institute, University of Groningen, Groningen, Netherlands, associated to ³⁸

⁷⁹ Universiteit Maastricht, Maastricht, Netherlands, associated to ³⁸

⁸⁰ Tadeusz Kosciuszko Cracow University of Technology, Cracow, Poland, associated to ⁴¹

⁸¹ Universidad de Coruña, A Coruña, Spain, associated to ⁴⁵

⁸² Department of Physics and Astronomy, Uppsala University, Uppsala, Sweden, associated to ⁶⁰

⁸³ University of Michigan, Ann Arbor, MI, United States, associated to ⁶⁹

^a Centro Federal de Educação Tecnológica Celso Suckow da Fonseca, Rio De Janeiro, Brazil

^b Center for High Energy Physics, Tsinghua University, Beijing, China

^c Hangzhou Institute for Advanced Study, UCAS, Hangzhou, China

^d School of Physics and Electronics, Henan University , Kaifeng, China

^e LIP6, Sorbonne Université, Paris, France

^f Lamarr Institute for Machine Learning and Artificial Intelligence, Dortmund, Germany

^g Universidad Nacional Autónoma de Honduras, Tegucigalpa, Honduras

^h Università di Bari, Bari, Italy

ⁱ Università di Bergamo, Bergamo, Italy

^j Università di Bologna, Bologna, Italy

^k Università di Cagliari, Cagliari, Italy

^l Università di Ferrara, Ferrara, Italy

^m Università di Genova, Genova, Italy

ⁿ Università degli Studi di Milano, Milano, Italy

^o Università degli Studi di Milano-Bicocca, Milano, Italy

^p Università di Padova, Padova, Italy

^q Università di Perugia, Perugia, Italy

^r Scuola Normale Superiore, Pisa, Italy

^s Università di Pisa, Pisa, Italy

^t Università della Basilicata, Potenza, Italy

^u Università di Roma Tor Vergata, Roma, Italy

^v Università di Siena, Siena, Italy

^w Università di Urbino, Urbino, Italy

^x Universidad de Alcalá, Alcalá de Henares , Spain

^y Facultad de Ciencias Físicas, Madrid, Spain

^z Department of Physics/Division of Particle Physics, Lund, Sweden

[†] Deceased